

QUALITATIVE STUDY of the EFFECT of a COMPARTMENT

ENCLOSURE on FIRE PLUME ENTRAINMENT

by

Scott Kenneth Anderson

A Master's Thesis

Submitted to the Faculty

of the

WORCESTER POLYTECHNIC INSTITUTE

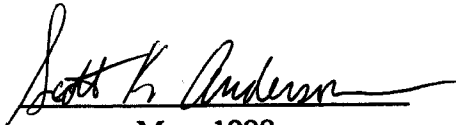
in partial fulfillment of the requirements for the

Degree of Master of Science

in

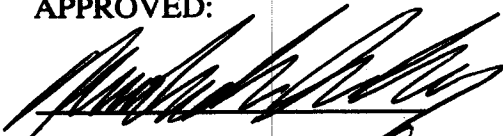
Fire Protection Engineering

by

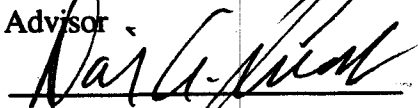


May, 1998

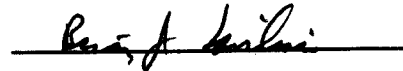
APPROVED:



Professor Nicholas A. Dembsey
Advisor



Professor David A. Lucht, Director
Center for Firesafety Studies



Professor Brian J. Savilonis
Reader

Abstract

Zone models are a widely used tool in fire protection engineering used to predict how fires will develop in compartments. Zone models such as CFAST, use fire plume entrainment algorithms for plumes in the open. Under which fire to compartment size conditions the effect of the enclosure influences plume entrainment is currently unclear. The accuracy of zone model mass flow simulations can be improved if the conditions of enclosure influence are known and appropriate entrainment algorithms are developed. This work was a systematic study of six global parameters that effect flame height and the enclosure effect on fire plume entrainment, exclusive of the door jet. A series of experiments was conducted using the 50% intermittancy flame heights of gas burner fires both inside and outside of a compartment as a qualitative measure of fire plume entrainment. Two propane fueled gas burners, one square measuring 0.3m by 0.3m, and one rectangle measuring 0.6m by 0.3m, were used to supply propane flow rates ranging from 20kW to 150kW. The compartment that was used measures 2.4m by 3.6m in plan by 2.4m in height with a door vent 2.0m by 0.76m centered on one of the short walls. The burner was located in the center of the compartment with its top surface 0.6m above the floor to avoid door jet effects on the flames. A thermocouple tree, located in the front of the burner, was used to measure vertical temperature profiles. The gas layer interface was measured visually. The width of the compartment was narrowed from 2.4m to 0.76m, the length of the compartment was also decreased from 3.6m to 1.25m and the height was lowered from 2.4m to 1.5m to obtain various ratios of compartment size to gas burner width (0.3m). Over the range of compartments and fire sizes tested no enclosure effect was found. However, it was found that the convective heat release rate of the fire

should be used instead of the total heat release rate when comparing different fuels. The measured flame heights showed good correlation to the flame height expressions of Zukoski and Heskestad when modified to use the convective heat release rate.

Acknowledgements

I would like to thank Professor Nicholas A. Dembsey for his help and guidance, Professor Brian J. Savilonis, all of the faculty at the Center for Firesafety Studies, Christopher J. Wieczorek for his help in conducting the experiments and Steve Derosier for help in constructing the experimental equipment. Most of all I would like to thank my girlfriend, Karen, and my family for their support that has helped me to finish this project.

My thanks also go to the National Science Foundation whose Graduate Research Traineeship Grant # EEC-9256999 partially supported this work.

Table of Contents	
ABSTRACT	ii
ACKNOWLEDGEMENTS	iv
LIST OF FIGURES	vii
LIST OF TABLES	x
NOMENCLATURE	xi
1.0 INTRODUCTION	1
1.1 BASIC COMPARTMENT DYNAMICS	3
2.0 BACKGROUND	6
2.1 ZONE MODELS	6
2.2 FLAME HEIGHT CORRELATIONS	6
2.2.1 Flame Height Intermittency	7
2.2.2 Flame Puffing – Pagni	7
2.2.3 Zukoski	7
2.2.4 Heskestad	8
2.3 COMPARTMENT FIRE PLUME ENTRAINMENT	8
2.3.1 Hasemi and Tokunaga	9
2.3.2 Steckler, Quintiere and Rinkinen	9
2.3.3 Kolb, Audouin, Most and Torero	10
2.3.4 Dembsey, Pagni and Williamson	10
2.4 UPPER LAYER TEMPERATURE CORRELATION	11
3.0 EXPERIMENTAL APPARATUS	13
3.1 TEST COMPARTMENT	13
3.2 PROPANE GAS DELIVERY SYSTEM	13
3.3 GAS BURNERS	17
3.4 VIDEO CAMERA	20
4.0 EXPERIMENTAL PROCEDURE	21
4.1 COMPARTMENT CONFIGURATIONS	24
5.0 EXPERIMENTAL DATA	30
5.1 FLAME PUFFING - DATA	32
5.2 FLAME INTERMITTENCY	32
5.3 BASELINE – EXPERIMENTS IN THE OPEN	34
5.3.1 Comparison of Baseline to Zukoski’s Correlation	36
5.3.2 Comparison of Baseline to Heskestad’s Correlation	37
5.3.3 Convective Heat Release Rate	38
5.4 COMPARISON OF BASELINE TO COMPARTMENT EXPERIMENTS	41

<i>5.4.1 Compartment Configurations #1 to #4</i>	41
<i>5.4.2 Compartment Configuration #5</i>	46
<i>5.4.3 Compartment Configuration #6</i>	50
<i>5.4.4 Compartment Configuration #7</i>	54
5.5 COMPARISON OF COMPARTMENT EXPERIMENTS TO DEMBSEY ET AL	57
6.0 CONCLUSIONS	65
7.0 FUTURE WORK	67
8.0 REFERENCES	68
9.0 APPENDIX A	70

List of Figures

Figure 1: Basic control volumes of a fire in a compartment. CV1 is the hot layer and CV2 is the cool layer.....	3
Figure 2: Schematic of flow around a burner in a compartment.	4
Figure 3: Schematic of the propane tank, regulator and load cell portion of the propane gas delivery system.	15
Figure 4: Schematic of the control panel used to regulate the flow of propane from the gas delivery system.....	16
Figure 5: Side view schematic of the square gas burner. The dotted line represents the kaowool blanket, which was used as the diffusive surface.....	18
Figure 6: Plan view schematic of the square gas burner. The burner is shown without kaowool on top.....	18
Figure 7: Side view schematic of the rectangular gas burner. The dotted line represents the kaowool blanket, which was used as the diffusive surface.....	19
Figure 8: Plan view schematic of the rectangular gas burner. The burner is shown with no kaowool on top.....	19
Figure 9: Plan view of compartment configuration #1, ceiling height 2.4m, and doorway height 2.0m, showing position of gas burner and thermocouple tree.	25
Figure 10: Plan view of compartment configuration #2, ceiling height 2.4m, and doorway height 2.0m, showing position of gas burner and thermocouple tree. Heavy lines indicate the new walls added to change the dimensions of the compartment.....	26
Figure 11: Plan view of compartment configuration #3, ceiling height 2.4m, and doorway height 2.0m, showing position of gas burner and thermocouple tree. Heavy lines indicate the new walls added to change the dimensions of the compartment.....	26
Figure 12: Plan view of compartment configuration #4, ceiling height 2.4m, and doorway height 2.0m, showing position of gas burner and thermocouple tree. Heavy lines indicate the new walls added to change the dimensions of the compartment. The dotted line indicates a cutoff of the rest of the compartment.....	27
Figure 13: Front view of compartment configuration #5, plan is the same as compartment configuration #4 with the ceiling height lowered to 1.5m. There is no soffet on the door. The burner was still located in the center of the room with the thermocouple tree located between the burner and the door.	27

Figure 14: Front view of compartment configuration #6, plan is the same as compartment configuration #4, ceiling height 1.5m with a 0.3m soffet on the door. The burner was still located in the center of the room with the thermocouple tree located between the burner and the door.	28
Figure 15: Plan view of compartment configuration #7, the front view was the same as compartment configuration #6 ceiling height 1.5m, and doorway height 1.2m, which was used for the experiments with the rectangular burner. Heavy lines indicate the new walls added to change the dimensions of the compartment. The dotted line indicates a cutoff of the rest of the compartment.	29
Figure 16: One second time interval of a 60kW fire on the square burner at 10 frames per second.	32
Figure 17: Normalized intermittency for all experiments conducted, including both burners and inside and outside of the compartment.	34
Figure 18: Flame heights from experiments on the square and rectangular burners in the open under the hood. These experiments make up the baseline for the compartment experiments.	35
Figure 19: Comparison of baseline experiments in the open conducted on the square burner and the correlation of Zukoski ⁵	36
Figure 20: Comparison of baseline experiments in the open conducted on the square burner and the correlation of Heskestad. ⁶ Error bars on Heskestad correlation are 20%.	37
Figure 21: Flame heights, measured and Cetegen et al. ⁹ , versus \dot{Q}_c^* , also included is the convective Zukoski correlation with $\gamma_c=3.5$	39
Figure 22: Comparison of measured flame heights in the open to convective Heskestad correlation, with error bars of 20%.	40
Figure 23: Flame height comparison of compartment configurations #1 to #4 to the baseline in the open. The flame height is plotted versus the non-dimensional convective heat release rate, \dot{Q}_c^*	44
Figure 24: Entrainment heights and flame heights for compartment configurations #1 to #4.	45
Figure 25: Comparison of measured upper layer gas temperatures for compartment configurations #1 to #4 to the values calculated by MQH. ¹³	46

Figure 26: Flame height comparison of compartment configurations #5 to the baseline in the open. The flame height is plotted versus the non-dimensional convective heat release rate, \dot{Q}_c^*	48
Figure 27: Entrainment heights and flame heights for compartment configuration #5.....	49
Figure 28: Comparison of measured upper layer gas temperatures for compartment configurations #1 to #5 to the value calculated by MQH. ¹³	50
Figure 29: Flame height comparison of compartment configuration #6 to the baseline in the open. The flame height is plotted versus the non-dimensional convective heat release rate, \dot{Q}_c^*	52
Figure 30: Entrainment heights and flame heights for compartment configuration #6.....	53
Figure 31: Comparison of measured upper layer gas temperatures for compartment configurations #1 to #6 to the value calculated by MQH. ¹³	54
Figure 32: Flame height comparison of compartment configuration #7 to the baseline in the open. The flame height is plotted versus the non-dimensional convective heat release rate, \dot{Q}_c^*	55
Figure 33: Entrainment heights and flame heights for compartment configuration #7.....	56
Figure 34: Comparison of measured upper layer gas temperatures for compartment configurations #1 to #7 to the value calculated by MQH. ¹³	57
Figure 35: Comparison of flame heights in the open and compartment configurations #1 to #7 to the actual data of Dembsey et al. ² and the convective Dembsey et al. correlation.	62
Figure 36: Comparison of the Upper layer gas temperatures of compartment configurations #1 to #7 and Dembsey et al. ² plotted versus heat release rate. The temperatures of compartment configuration #6 are high because the top thermocouple was possibly located in the ceiling jet. The high temperature in compartment configuration #7 is due to the small compartment size and the higher heat release rate.....	63
Figure 37: Comparison of burner side temperatures of Anderson to side wall temperatures of Dembsey et al. ²	64

List of Tables

Table 1: HRRs and \dot{Q}_D^* used in experiments on the square burner.....	21
Table 2: HRRs and \dot{Q}_D^* used in experiments on the rectangular burner.	21
Table 3: Geometric compartment and burner parameters for all seven compartment configurations and Dembsey et al.'s ² compartment.....	25
Table 4: Flame height data for all tests performed including the hydraulic diameter of the burner, heat release rate, non-dimensional heat release rate, 50% intermittency height, 50% intermittency height normalized by the hydraulic diameter, slope of the intermittency curve divided by Z(50), and flame pulsing.	31
Table 5: Comparison of Entrainment rates and burner side induced flows for the Dembsey et al. ² experiments and the four experiments where the burner side temperatures were measured in this study.....	61

Nomenclature

- A_0 = area of door vent (m^2)
 A_b = area of the burner (m^2)
 A_T = interior surface area of compartment (m^2)
 C_p = specific heat (kJ/kg K)
 $D = 4A_b/P_b$ = hydraulic diameter (m)
 $D_e = (4A_b/\pi)^{1/2}$ = area equivalent diameter (m)
 f = pulsing frequency of flame (Hz)
 $g = 9.81 m/s^2$ = gravity
 Gr = Grashof Number
 h_k = effective heat transfer coefficient (kW/mK)
 H = ceiling height (m)
 H_0 = height of door vent (m)
 ΔH_c = heat of combustion (MJ/kg)
 k = thermal conductivity of compartment surface (kW/mK)
 \dot{m} = flow up hot burner side per unit perimeter (kg/ms)
 \dot{m}_e = mass entrainment rate (kg/s)
 \dot{m}_f = mass flow rate of fuel from fire (kg/s)
 \dot{m}_g = mass flow rate of gas out of compartment (kg/s)
 n = constant in flame height correlation
 $N = [(C_p T_{amb}) / (g \rho_{amb}^2 (\Delta H_c / r)^3)] (\dot{Q}^2 / D^5)$
 $N_C = [(C_p T_{amb}) / (g \rho_{amb}^2 (\Delta H_c / r)^3)] ((\alpha \dot{Q})^2 / D^5)$
 P_B = perimeter of the burner (m)
 P_C = perimeter of the compartment (m)
 Pr = Prandtl Number
 \dot{Q} = fire heat release rate (kW)
 $\dot{Q}_C^* = \alpha \dot{Q} / (\rho_{amb} C_p T_{amb} (gD)^{1/2} D^2)$
 $\dot{Q}_D^* = \dot{Q} / (\rho_{amb} C_p T_{amb} (gD)^{1/2} D^2)$
 t = exposure time (s)
 t_p = thermal penetration time (s)
 T_{amb} = ambient air temperature (K)
 T_{gl} = lower layer gas temperature (K)
 T_{gu} = upper layer gas temperature (K)
 Z = height in wall flow calculations (m)
 Z_e = entrainment height (m)
 Z_i = intermittent flame height (m)
 Z_{in} = interface height (m)
 Z_{50} = mean flame height, 50% intermittency (m)
 α = convective fraction of fuel
 $\beta = 1/T$ (1/K) = buoyancy term
 δ = thickness of compartment surface (m)

Δ = intermittency curve slope thickness

γ = constant in flame height correlation

γ_c = modified constant in new flame height correlation

ν = kinematic viscosity (m^2/s)

ρ_{amb} = ambient air density (kg/m^3)

1.0 Introduction

Performance based codes are being developed to augment the prescriptive codes that are used currently for designing building fire and life safety systems. For performance based codes to become a reality, fire protection engineers need to be able to accurately calculate how a fire develops in a building and how that building reacts to the fire. Zone models¹ are used by engineers to simulate fire environments in compartments. Zone models are only as good as the flame height and entrainment correlations that they use. In order to make zone models as accurate as possible, it must be determined what effect the compartment has on a fire and account for that effect in any correlation used.

Limited work has been performed studying the enclosure effect of a compartment on fire plume entrainment. Dembsey et al.² performed a series of experiments involving large fires in a compartment where a potential compartment effect was observed. That set of experiments is the impetus for this study.

This work is a systematic study that addresses the enclosure effect of a compartment on fire plume entrainment. Flame height is used as a qualitative measure of entrainment. Entrainment is directly related to flame height, in that if entrainment is enhanced at every level then the flame will not need to burn as high to gather enough oxygen to combust the fuel. Conversely, if entrainment is hindered then the flame will need to burn higher to be able to gather enough oxygen.

This systematic study investigated four global parameters directly related to enclosure effect: 1. The ratio of the size of the compartment to the size of the vent, quantified as $A_T/A_0\sqrt{H_0}$, where A_T is the interior surface area of the compartment, A_0 is the area of the door vent and H_0 is the height of the door vent. 2. The tightness of the

compartment around the burner, quantified by the ratio of the perimeter of the compartment to the perimeter of the burner, P_C/P_B . 3. Entrainment height, Z_e , which is the distance between the base of the flame and the gas layer interface. 4. Upper layer gas temperature, T_{gu} . In addition two global parameters related to flame height were studied 1. Convective Fraction of the fuel and 2. Burner construction.

Experiments were performed both in the open and inside a compartment that measures 2.4m x 3.6m in plan x 2.4m in height, with a 2.0m x 0.76m door vent. In order to study the first two parameters the size of the compartment was systematically decreased around the burner. The ceiling height of the compartment was lowered from 2.4m to 1.5m. The upper layer gas temperatures were measured with a thermocouple tree located in the room. The burner shapes and hydraulic diameter (D) were studied in a controlled manner along with enclosure effect. The experiments were performed with a propane gas delivery system designed to make flames with heat release rates (HRRs) ranging from 20kW to 150kW. The propane gas delivery system supplied the fuel to two porous surface burners, a square burner 0.3m x 0.3m and a rectangular burner 0.6m x 0.3m. The cutoff for an experiment to be considered residential full scale; i.e. fully turbulent flames, is a hydraulic diameter of 0.3m.³ Both burners used met this criteria for fully turbulent flames.

1.1 Basic Compartment Dynamics

Three of the four global parameters chosen for the systematic study of a compartment effect are all taken from basic compartment dynamics. The fire environment in a compartment can be divided into two control volumes, see Figure 1.

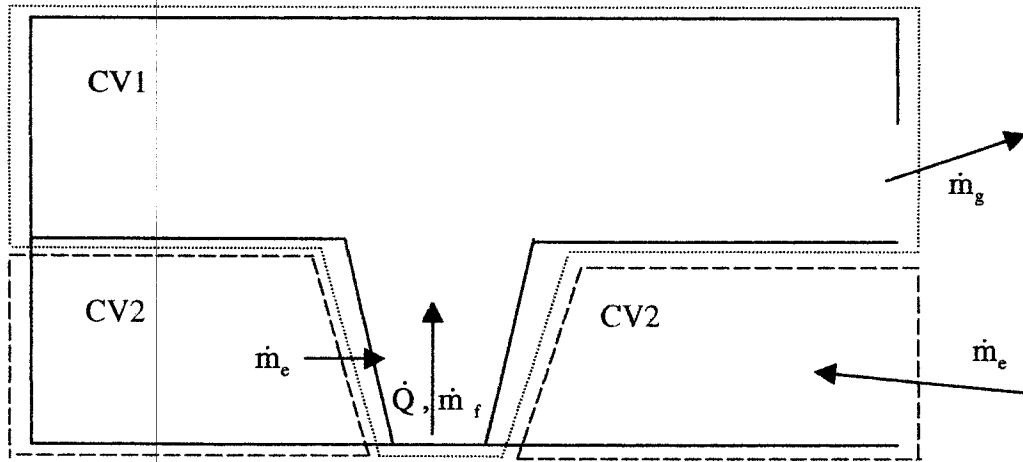


Figure 1: Control volumes for a fire in a compartment. CV1 is the hot layer and fire plume, CV2 is the cool layer, \dot{m}_g is the gas flow rate out of the compartment, \dot{m}_f is the mass flow rate of fuel from the fire and \dot{m}_e is the mass entrainment rate.

The parameters $A_r/A_0\sqrt{H_0}$ and T_{gu} are taken from a simple energy balance on CV1: $\dot{Q} = \dot{m}_g c_p \Delta T + h_k A_r \Delta T$, where \dot{m}_g is mass flow rate of gas out of the compartment, h_k is the effective heat transfer coefficient, \dot{Q} is the total HRR of the fire and ΔT is the difference between the upper and lower layer temperature all other variables are in the Nomenclature. The variable \dot{m}_g is proportional to $A_0\sqrt{H_0}$, the relationship can be derived from Bernoulli's equation.⁴ From manipulation of the energy balance, $\Delta T/T_0 = ((\dot{Q}/c_p T_0 \dot{m}_g)/(1 + (h_k A_r/c_p \dot{m}_g)))$, the parameter $A_r/A_0\sqrt{H_0}$ can be obtained. The upper layer temperature rise in the compartment is important because radiation from

the upper layer supplies heat to the lower walls and floor of the compartment. The heating of the lower walls and floor effects the flow patterns in the lower layer.

The parameter entrainment height, Z_e , can be taken from a mass balance on CV1:

$\dot{m}_g = \dot{m}_e + \dot{m}_f$, where \dot{m}_e is the mass entrainment rate and \dot{m}_f is the mass flow rate of the fuel into CV1. The variable \dot{m}_e is directly related to the entrainment height, Z_e .

The parameter P_d/P_b is relevant to the tightness of the compartment around the burner. The flame entrains air, from all sides in the lower layer, which flows in from the door vent, see Figure 2. If the compartment constricts this flow then the entrainment will be altered.

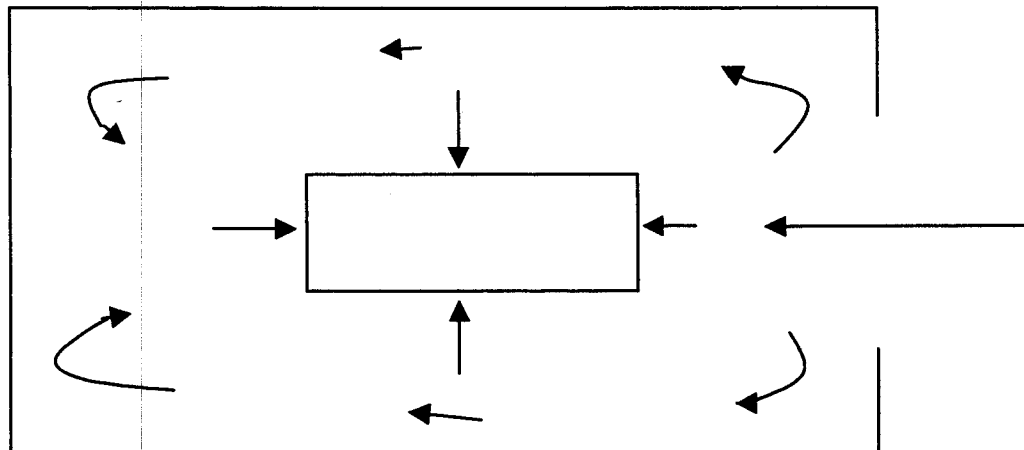


Figure 2: Schematic of flow around a burner in a compartment.

The two parameters related to flame height have been determined to be important through research of previous experiments. The parameter of burner construction is important because a consistent relationship between flame height and burner shape and construction has not been determined. Dembsey et al.² include a comprehensive list of flame height experiments performed on different shape burners and no consistent

correlation was found. The convective fraction of the fuel has been determined to be an important parameter by Heskestad⁵ and Delichatsios⁶, who both include it in the flame height analysis performed in their work.

2.0 Background

2.1 Zone Models

Zone models typically represent a compartment as two separate gas zones, a hot upper layer and a cool, lower layer.¹ During the fire, mass is pumped from the lower layer to the upper layer by the fire plume. Zone models calculate the amount of mass pumped by using a fire plume entrainment algorithm. CFAST⁷ is a widely used zone model developed by the National Institute of Standards and Technology. CFAST uses the McCaffrey plume algorithm to simulate mass flows. The fire plume entrainment algorithm used in CFAST, as with other zone models, is for fire plumes in the open and not for fire plumes in a compartment. The error that results from using a plume-in-the-open algorithm when simulating a plume in a compartment is not known and needs to be investigated to improve the accuracy of zone models such as CFAST.

2.2 Flame Height Correlations

Many investigators have correlated the heights of turbulent diffusion flames. Two that will be discussed in detail are the correlations of Zukoski⁸ and Heskestad⁹. Their flame height correlations were used as a reference in this study for comparison to the experimental data. The flame height data from experiments conducted in the open were directly compared to these correlations. Once this baseline was established the flame heights from the compartment experiments were compared to the baseline.

2.2.1 Flame Height Intermittency

The idea of intermittency¹⁰ was used to describe the height of the flames observed. Intermittency is defined as the fraction of time during which at least part of the flame lies above a horizontal plane located at a given elevation above the burner. In this project the focus was on the 50% intermittency flame height. This is the height at which the flame exists half of time. The 50% intermittency flame height is also approximately the eye average flame height. The flame height correlations discussed in this section are based on the 50% intermittency flame height.

2.2.2 Flame Puffing – Pagni

Pagni¹¹ developed a correlation for the frequency of the pulsing of a fire. Many different fuels were compared and the correlation is only dependant on the diameter of the fire and is applicable for $0.05\text{m} < D < 50\text{m}$:

$$f\sqrt{(D/g)} = 0.48 \pm 0.10 \quad (1)$$

Where f is the pulsing frequency (Hz), D is the hydraulic diameter (m) and g is gravity (9.81 m/s^2).

2.2.3 Zukoski

Zukoski's correlation is based on experiments performed by Cetegen et al.¹² A series of experiments measuring the heights of diffusion flames over a wide range of HRRs, using natural gas as a fuel were conducted. Three different sized circular burners, 0.10m, 0.19m and 0.50m in diameter, were used. The HRRs used ranged from 10kW to 200kW. Cetegen et al. determined the flame heights of these fires by recording the

experiments and analyzing the data frame by frame. Cetegen et al. then plotted the 50% intermittency flame height versus \dot{Q}_D^* , a non-dimensional HRR and obtained an equation for flame height of the form: $Z_{50}/D = 3.3\dot{Q}_D^{*2/3}$ for $\dot{Q}_D^* < 1$ and $Z_{50}/D = 3.3\dot{Q}_D^{*2/5}$ for $\dot{Q}_D^* > 1$. Where Z_{50} =50% intermittency flame height (m), $\dot{Q}_D^* = \dot{Q}/(\rho_{amb}c_pT_{amb}(gD)^{1/2}D^2)$, \dot{Q} =total HRR (kW) and D=hydraulic diameter of the burner. Zukoski's correlation is based on the total heat release rate of the fuel. Other variable definitions can be found in the Nomenclature.

2.2.4 Heskestad

Heskestad's⁹ correlation comes from data collected from a wide range of experiments. The fuels used included methane, ethylene, propane, butane, gasoline, JP-4 and wood cribs. Heskestad correlated these flame height data into the form: $Z_{50}/D_e = 15.6N^{1/5} - 1.02$ for $10^{-5} < N < 10^5$, where the non-dimensional heat release rate $N = [c_pT_{amb}/g\rho_{amb}(\Delta H_c/r)^3]\dot{Q}^2/D_e^5$ and D_e =area equivalent diameter (m). To calculate D_e the area of the fire is used and an equivalent diameter is computed as if the fire was a circle. Heskestad's correlation is based on the total HRR of the fuel. Other variable definitions can be found in the Nomenclature.

2.3 Compartment Fire Plume Entrainment

The majority of research performed on compartment fires has been to study the direct effect of walls and corners on fire plume entrainment. The work of Hasemi and

Tokunaga¹³, Steckler et al.¹⁴, Kolb et al.¹⁵ and Dembsey et al.² will be discussed as to how their research applies to enclosure effect.

2.3.1 Hasemi and Tokunaga

Hasemi and Tokunaga¹³ performed a study of wall and corner effects on flame height. This work did not include a study of the enclosure effect of the compartment. Hasemi and Tokunaga's research included flame height experiments in three different locations. A baseline study was conducted in a semi-infinite space, the same fires were then run against a wall and in a corner. Three square burners with hydraulic diameters of 0.5m, 0.3m and 0.2m were used in all locations. The experiments were recorded with a video camera and the data analyzed frame by frame to determine flame heights.

The baseline experiments conducted in the open matched Zukoski's⁸ correlation. When the fires were placed against the wall the flame height increased. The value of γ rose from 3.3 to 3.5. This increase in flame height indicates that the wall hindered the fire plume entrainment. The corner position hindered the entrainment to a greater degree increasing the flame height further, γ increased to 4.3. For all experiments the values of n matched Zukoski.⁸

2.3.2 Steckler, Quintiere and Rinkinen

Steckler, Quintiere and Rinkinen¹⁴ studied the flows induced by a fire in a compartment. They did not study the flame heights of these fires, but instead measured the door flows that were caused by fires in various compartment locations. The locations included center, sidewall and corner. Two different burner heights were tested at each

location, one flush to the floor and one 0.3m above the floor. Over the ranges of positions and heights tested, they found similar results to Hasemi and Tokunaga.¹³ The largest change in entrainment came when the fire was moved from the center of the compartment into the corner position. Only a slight change in entrainment was found with the fire against a wall.

2.3.3 Kolb, Audouin, Most and Torero

Kolb et al.¹⁵ performed a study of confinement effect on the height of buoyant diffusion flames. A propane gas burner, measuring 0.25m x 0.40m, was placed in a horizontal channel. The channel could be manipulated to control the air entrainment (level of confinement) into the fire by adding or removing floor panels. Kolb et al. found similar results to Hasemi and Tokunaga¹³ and Steckler et al.¹⁴ The results showed that the flame height was dependant on the level of entrainment, increasing when the channel hindered entrainment (closed floor).

2.3.4 Dembsey, Pagni and Williamson

Dembsey et al.² performed a series of experiments studying near-field entrainment of compartment fires. Near-field entrainment occurs when the hot layer interface is below the mean flame height so that cold layer entrainment only occurs near the burner surface. Twenty full scale, near field experiments were conducted in a standard test compartment measuring 2.5m x 3.7m in plan x 2.5m with 2.0m x 0.76m door vent. The propane fired porous surface burner used in the experiments was a rectangle measuring 0.61m x 1.22m. Of the 20 experiments 8 were in a sidewall configuration and 12 were in

the center of the room. The heat release rates of the fires ranged from 330kW to 980kW. Based on the analysis of the observed flame heights the following correlation was developed: $Z_{50}/D = 1.2\dot{Q}_D^{*2/3}$ for $0.5 < \dot{Q}_D^* < 1$ and $Z_{50}/D = 1.2\dot{Q}_D^{*2/5}$ for $1 < \dot{Q}_D^* < 1.5$. The near-field experiments showed a flame height decrease of 64% in γ when compared to Zukoski's⁸ correlation for fires in the open. Dembsey et al.² investigated many flame heights in the open correlations and found that their flame heights were much lower than those found by previous researchers. Additionally, the various correlations investigated did not show a consistent effect of HRR, D and burner shape on flame height. Dembsey et al.'s experiments were only performed inside a compartment and not in the open for the same burner fires. Therefore other variables such as HRR, D and burner shape are confounded in the results.

2.4 Upper Layer Temperature Correlation

McCaffrey, Quintiere, and Harkleroad¹⁶ (MQH) developed a correlation for predicting the upper layer gas temperature in a compartment during a fire. The MQH correlation was developed from a simple energy balance on the upper layer and correlation to experimental data. Over 100 experimental fires were analyzed for the correlation. The ceiling heights of the compartment ranged from 0.3m to 2.7m. The floor areas ranged from 0.14m² to 12.0m². The majority of the fires in the tests were located in the center of the compartment. The MQH correlation is accurate up to an upper layer temperature of 600°C. The analysis of the data led to the power law relationship:

$$\Delta T_g = 480 \left(\frac{\dot{Q}}{\sqrt{g c_p \rho_{amb} T_{amb} A_0 \sqrt{H_0}}} \right)^{2/3} \left(\frac{h_k A_T}{\sqrt{g c_p \rho_{amb} A_0 \sqrt{H_0}}} \right)^{-1/3} \quad (2)$$

where ΔT_g =upper gas temperature rise above ambient (K), A_T =total area of compartment enclosing surfaces (m^2), A_0 =area of opening (m^2), H_0 =height of opening (m) \dot{Q} =total HRR of the fire (kW) and h_k =effective heat transfer coefficient (kW/mK) which needs to be calculated based on the wall characteristics of the room. The heat transfer coefficient is calculated in one of two ways depending on whether the time of interest is less than or greater than the thermal penetration time, $t_p = (\rho c_p / k)(\delta/2)^2$, where k , ρ and c_p are the thermal properties for the compartment walls and δ is the thickness. To calculate h_k for times less than the thermal penetration time, $h_k = (k \rho c_p / t)^{1/2}$. If the time is greater than the thermal penetration time, $h_k = k / \delta$. All other symbols can be found in the Nomenclature.

3.0 Experimental Apparatus

3.1 Test Compartment

The test compartment used in the experiments was similar to the standard fire test compartment. The compartment measured 3.6m x 2.4m in plan x 2.4m in height. There was one door vent measuring 2.0m by 0.76m, centered on one of the short walls. The walls, ceiling and floor were all covered with 3 layers of 1.6cm (5/8") firecode sheet rock. The room was placed next to a large-scale hood, measuring 2.4m by 2.4m, to collect the products of combustion. The hood has a maximum flow rate of 4.69m³/s. A thermocouple tree was located in the room, between the burner and the door vent, to measure the gas temperature gradient from floor to ceiling during the tests. For compartment configurations #1 to #6, five thermocouples were spaced evenly from floor to ceiling. For compartment configurations #6 with the flush burner sides and #7, three thermocouples were spaced from floor to ceiling and two were used to measure the temperature of the walls and the burner sides. The thermocouples used in the experiments were K type and had a sampling rate of 0.2Hz. The burner side temperatures were only measured when flush the flush sides were on the burner. The compartment size was systematically decreased using extra walls. The extra walls were constructed of wood studs and one layer of 1.6cm (5/8") firecode sheet rock. The compartment configurations used can be seen in Figures 7 to 13.

3.2 Propane Gas Delivery System

The propane gas delivery system was designed to produce heat release rates up to 150kW for a duration of 10 minutes. The propane used for fuel had the following

properties: a molecular weight of 44 kg/kgmole, a density of 2.07 kg/m^3 at a pressure of $1.15 \times 10^5 \text{ Pa}$ (16.7PSIA) and a temperature of 21°C , a heat of combustion of 46.3 kJ/g and a purity of 96%. Three different size tanks, 9.1, 13.6 and 45.4kg (20, 30, 100 lb.), were used depending on the size of the fire desired. A pressure regulator was attached to the propane tank to control the pressure of the discharge from the tank. The regulator was attached to the propane tank by a CGA-510 connector. When a 45.4kg propane tank was being used a F181 excess flow valve was attached in place of the CGA-510 connector. The pressure regulator was manufactured by Matheson, model #3537-510, which has a maximum inlet pressure of $2.1 \times 10^7 \text{ Pa}$ (3000PSIG), a maximum flow rate of $0.0017 \text{ m}^3/\text{s}$ (215SCFH) of N_2 at $1.7 \times 10^7 \text{ Pa}$ (2500PSIG), and an operating temperature range of -40°C to 74°C . A load cell was used to measure mass loss, which allowed the measured propane flow rate at the rotometer to be checked. A schematic of this setup can be seen in Figure 3.

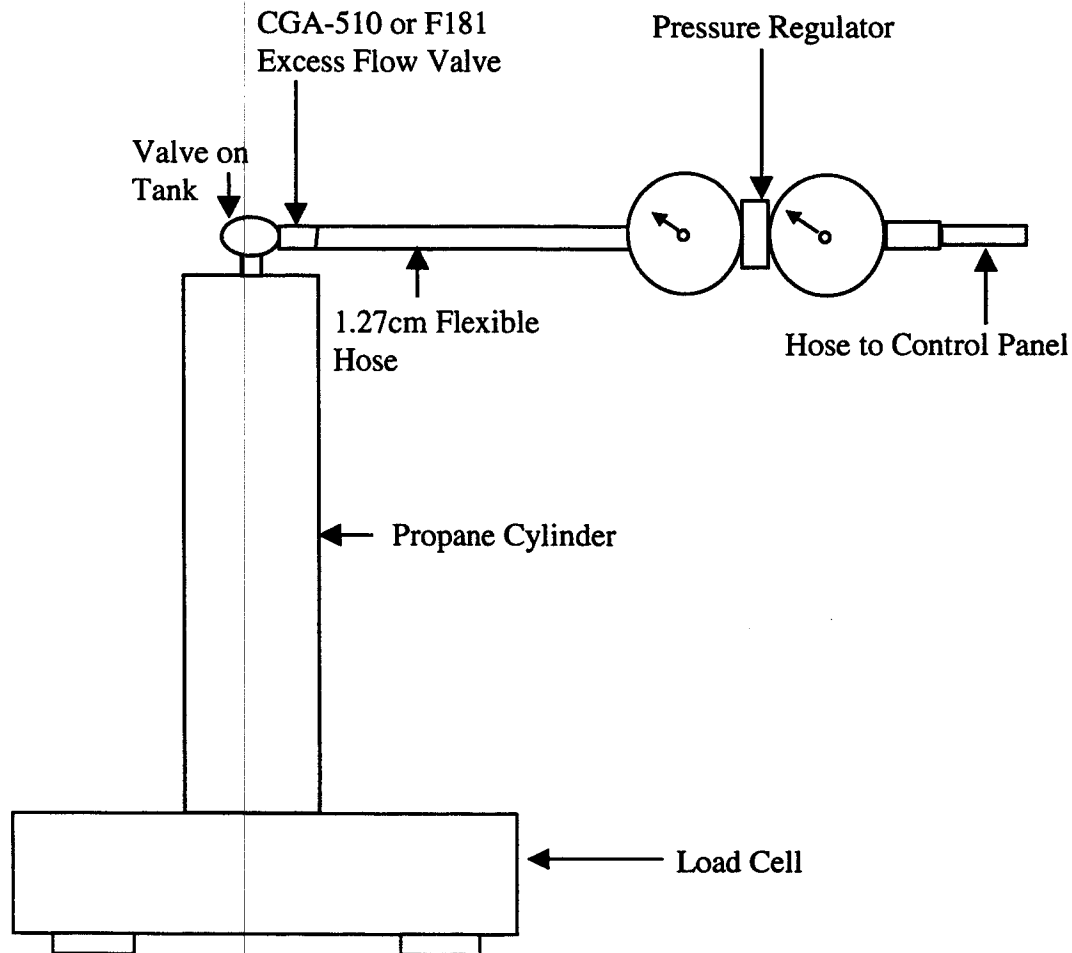


Figure 3: Schematic of the propane tank, regulator and load cell portion of the propane gas delivery system.

The remaining section of the propane gas delivery system was the control panel. The control panel regulates the flow of the fuel to the burner. The control panel has three parts, a ball valve, a rotometer and a needle valve. The ball valve manufactured by Whitey Co., model #B63TS8, was used as an on/off control for flow to the rotometer. The ball valve has a temperature rating of -54°C to 232°C , a pressure rating of $5.5 \times 10^6 \text{Pa}$ (800PSIG), a fully open valve coefficient, C_v , of 5.0 and an orifice size of 10.4mm. The

rotometer was used to measure the flow of the propane to the burners. The rotometer was manufactured by Bailey, Fisher and Porter Co. The maximum flow rate through the rotometer was $0.003\text{m}^3/\text{s}$ (5.93scfm) of air. The total pressure drop across the rotometer at maximum flow was 40.1cm (15.8”) of water column. The rotometer was accurate to within $\pm 2\%$. The needle valve manufactured by Whitey Co., model #B-1RS8, was located downstream from the rotometer and was used to set the flow rate of the fuel. The needle valve has a temperature rating of -54°C to 204°C , a pressure rating of $2.1 \times 10^7\text{Pa}$ (3000PSIG) at 38°C , a fully open valve coefficient, C_v , of 0.73 and an orifice size 6.4mm. A schematic of the control panel can be seen in Figure 4.

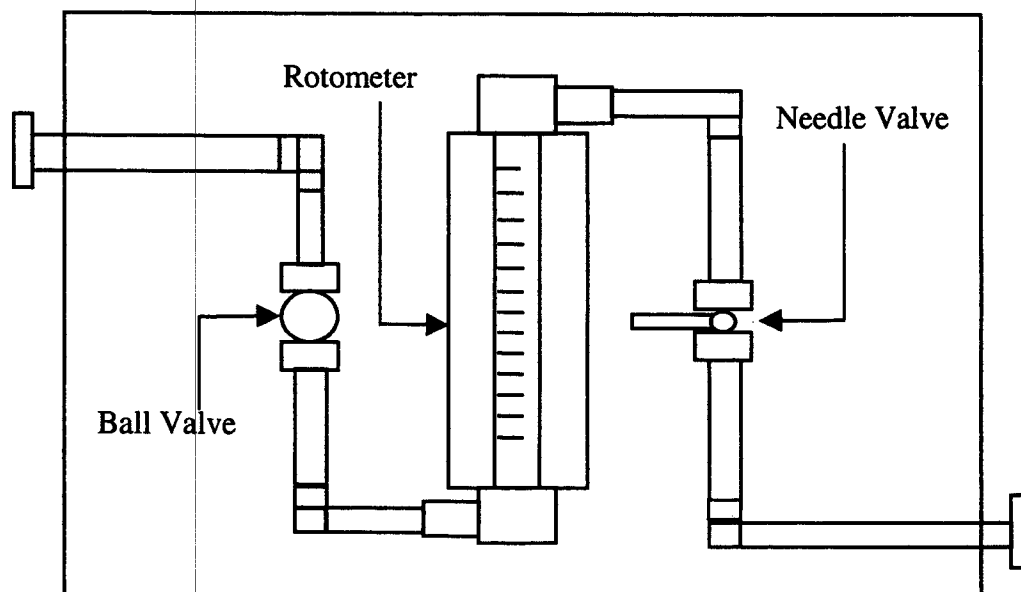


Figure 4: Schematic of the control panel used to regulate the flow of propane from the gas delivery system.

3.3 Gas Burners

Two gas burners were constructed: square 0.30m x 0.30m, see Figures 5 and 6, and rectangular 0.30m x 0.60m, see Figures 7 and 8. The hydraulic diameters of the burners were 0.3m and 0.4m respectively. The burners were constructed of 6mm (1/4") plate steel. Both burners had a 2.54cm (1") lip around the top surface, see Figures 5 and 7. The burners had a porous top surface used to diffuse the propane. The porous surface consisted of a 2.54cm (1") thick piece of kaowool blanket. The kaowool was clamped to the top surface of the burners with a metal brace that was screwed to the lip of the burners. In order to eliminate the lip in some experiments, 1.77cm (1/2") of ceramic fiberboard was attached to the sides of the burner creating a flush surface from the floor to the surface of the burner. The burners were connected to the propane delivery system by heat resistant 1.77cm (1/2") i.d. tubing. In order to avoid a door jet effect² the surface of the burner was located 0.61m above the floor.

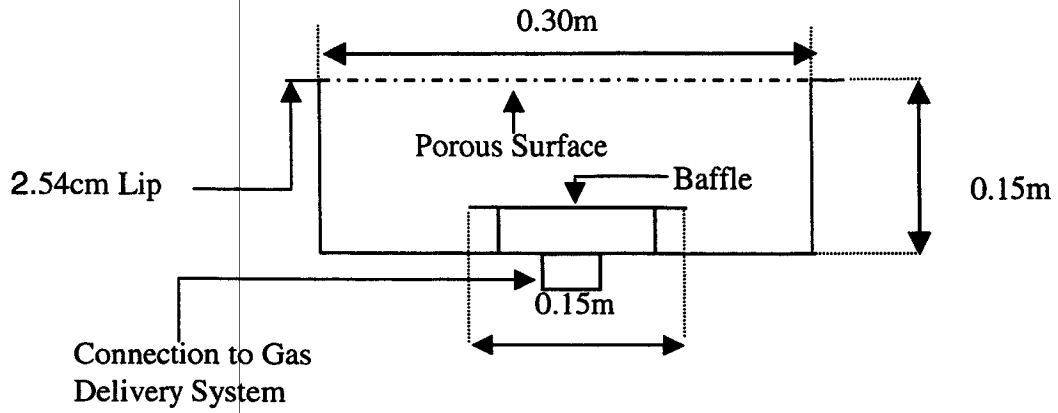


Figure 5: Side view schematic of the square gas burner. The dotted line represents the kaowool blanket, which was used as the diffusive surface.

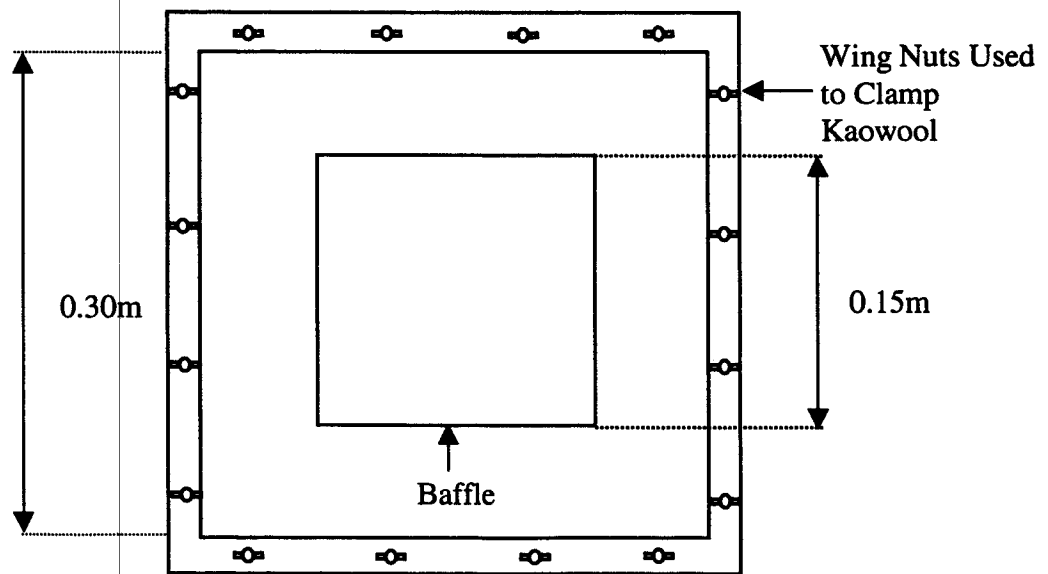


Figure 6: Plan view schematic of the square gas burner. The burner is shown without kaowool on top.

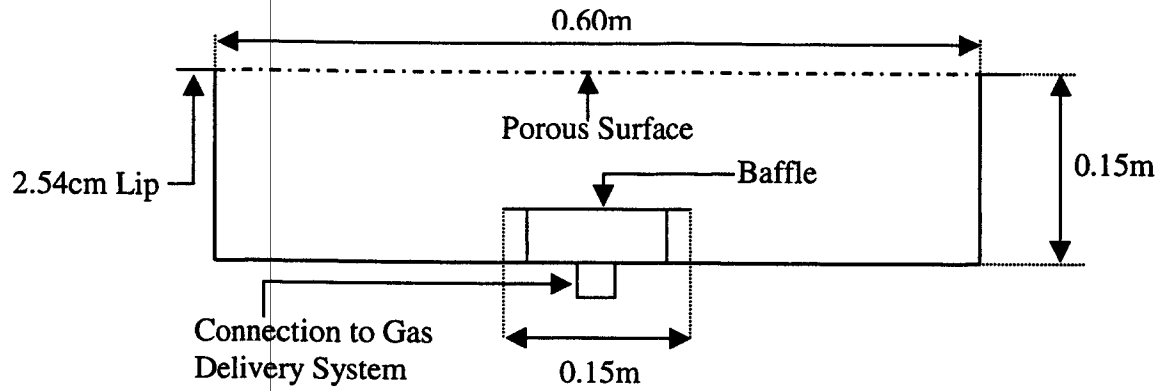


Figure 7: Side view schematic of the rectangular gas burner. The dotted line represents the kaowool blanket, which was used as the diffusive surface.

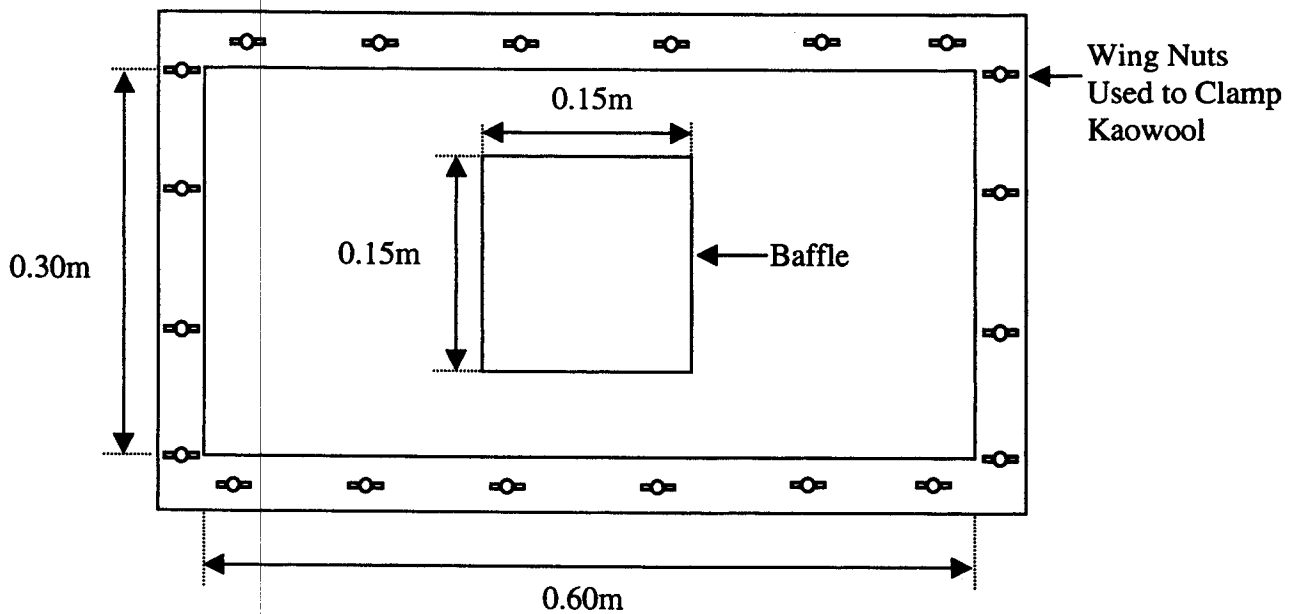


Figure 8: Plan view schematic of the rectangular gas burner. The burner is shown with no kaowool on top.

3.4 Video Camera

A video camera was used to record the flame height experiments. The camera was manufactured by Hitachi, model#2700A. The video camera recorded at a rate of 30 frames per second.

4.0 Experimental Procedure

The first step in performing a systematic study of enclosure effect is to establish a baseline that can be used as a comparison for the compartment data. The baseline for this study was a set of eight fires run in the open on the square burner under the hood, six of the experiments were on the original burner and two HRR's were repeated with flush sides on the burner. Four different HRRs were also run on the rectangular burner, two with flush sides and two without. The HRRs were chosen so that \dot{Q}_D^* would cover the range of Zukoski's correlation⁸. For the square burner three of the six \dot{Q}_D^* were less than 1 and three were greater than 1, see Table 1. For the rectangular burner one \dot{Q}_D^* was less than 1 and one was greater than 1, see Table 2.

Table 1: HRRs and \dot{Q}_D^* used in experiments on the square burner.

Heat Release Rate (kW)	\dot{Q}_D^*
20	0.37
30	0.55
40	0.73
60	1.1
70	1.28
80	1.46

Table 2: HRRs and \dot{Q}_D^* used in experiments on the rectangular burner.

Heat Release Rate (kW)	\dot{Q}_D^*
80	0.71
150	1.34

After the baseline was established the fires were moved into the 7 different compartment configurations, see Figures 9 to 15, to check for an enclosure effect. The square burner was run in compartment configurations #1 to #6 and the rectangular burner was run in compartment configuration #7 only. Each compartment experiment was run for approximately 10 minutes to allow a quasi-steady state to develop.

The primary piece of data collected during the experiments was the flame height of each of the fires. The flame height was recorded using a video camera. The video taped flames were then analyzed frame by frame, 450 frames per experiment, to assemble a flame intermittency chart. Three 150 frame sections were taken from random time intervals for each experiment, for experiments in the compartment all data was collected after the half way point of the experiment to ensure that the compartment had reached a quasi-steady state. For each frame analyzed the peak height of the continuous flame was recorded. The height of the flame was measured with a large ruler, which was placed next to the burner. Any detached "puff" of flame was not counted in the height. The length of time of the 150 frame intervals was chosen because it covered a span of approximately 40 flame puffs. The puffing frequency was calculated using the flame height versus time charts, which can be found in Appendix A. The frequency was computed by counting the number of peaks, each of which represented a puff, and then dividing by the time.

Other data collected during each experiment includes the gas temperature profile in the compartment. A tree consisting of five thermocouples was placed in the compartment centered between the burner and the door vent. The temperature profile

was used to calculate the interface height. The formulas used to calculate the interface height were taken from the work of Dembsey et al.²:

$$\int_0^H (T_g^{-1}) dz = [H - z_i] T_{gu}^{-1} + z_i T_{gl}^{-1} \quad (3)$$

$$\int_0^H (T_g) dz = [H - z_i] T_{gu} + z_i T_{gl} \quad (4)$$

where H=height of the compartment (m), T_g =gas temperature profile (K), z_i =interface height (m), T_{gu} =average upper layer gas temperature (K) and T_{gl} =average lower layer gas temperature (K). These formulas can be used to solve for the lower layer gas temperature and the interface height if the upper layer gas temperature is known. The average upper layer gas temperature can be estimated by taking an average of the values from the thermocouples located in the upper layer. The interface height was also recorded visually during testing. The visual estimate of the interface height was taken from a ruler, which was drawn on the wall of the compartment. The interface height fluctuated and thus has an error of ± 0.05 m. Due to the limited number of thermocouples in the compartment it was felt that the visual estimate of the interface height was more accurate, so the visual estimate was used for all entrainment height calculations.

The mass loss of propane was recorded using a load cell along with the duration of the experiment. The mass loss rate was used to calculate the heat release rate of the fire. The mass loss was divided by the duration of the experiment to determine the mass loss rate, then the mass loss rate was multiplied by the heat of combustion of the fuel. This calculated value was then multiplied by the purity to obtain the HRR of the fire.

4.1 Compartment Configurations

Seven different compartment configurations were evaluated. The two global parameters relating to the compartment are $A_T/A_0\sqrt{H_0}$ and P_c/P_B . $A_T/A_0\sqrt{H_0}$ was used to quantify the ratio of the size of the compartment to the size of the vent. This variable was important because the ratio represents how much air the fire can pull into the room compared to the size of the compartment. P_c/P_B is the ratio of the perimeter of the compartment to the perimeter of the burner. This variable was used to measure the confinement of the burner by the compartment. Six compartments for the square burner and one compartment for the rectangular burner were evaluated. The compartment size was decreased progressively throughout the experiments. The width and length of the compartment were decreased from compartment configurations #1 to #4, see Figures 9 to 12, until P_c/P_B matched the value from the experiments of Dembsey et al.², see Table 3. Next the global parameters upper layer temperature, T_{gu} , and entrainment height, Z_e were studied. In the experiments of Dembsey et al. very high upper layer gas temperatures were observed in the compartment and all entrainment was in the near field. To simulate those conditions the ceiling height was lowered to 1.5m for compartment configurations #5 and #6, see Figures 13 and 14, and Table 3. The lower ceiling height decreased the size of the door vent, which forced T_{gu} to increase. The lower ceiling height also decreased the entrainment height available to the fire plume. Compartment configuration #7 used for the rectangular burner had the same P_c/P_B ratio as compartment configurations #4 to #6 and the same ceiling height as configurations #5 and #6, see Figure 15 and Table 3.

Table 3: Geometric compartment and burner parameters for all seven compartment configurations and Dembsey et al.'s² compartment.

	$A_T/A_0\sqrt{H_0}$	P_c/P_B
	($m^{-0.5}$)	
Compartment Configuration #1	20.73	10.0
Compartment Configuration #2	16.26	6.7
Compartment Configuration #3	11.8	5.3
Compartment Configuration #4	4.68	3.4
Compartment Configuration #5	4.75	3.4
Compartment Configuration #6	6.84	3.4
Compartment Configuration #7	11.25	3.4
Dembsey et al. ²	23.02	3.4

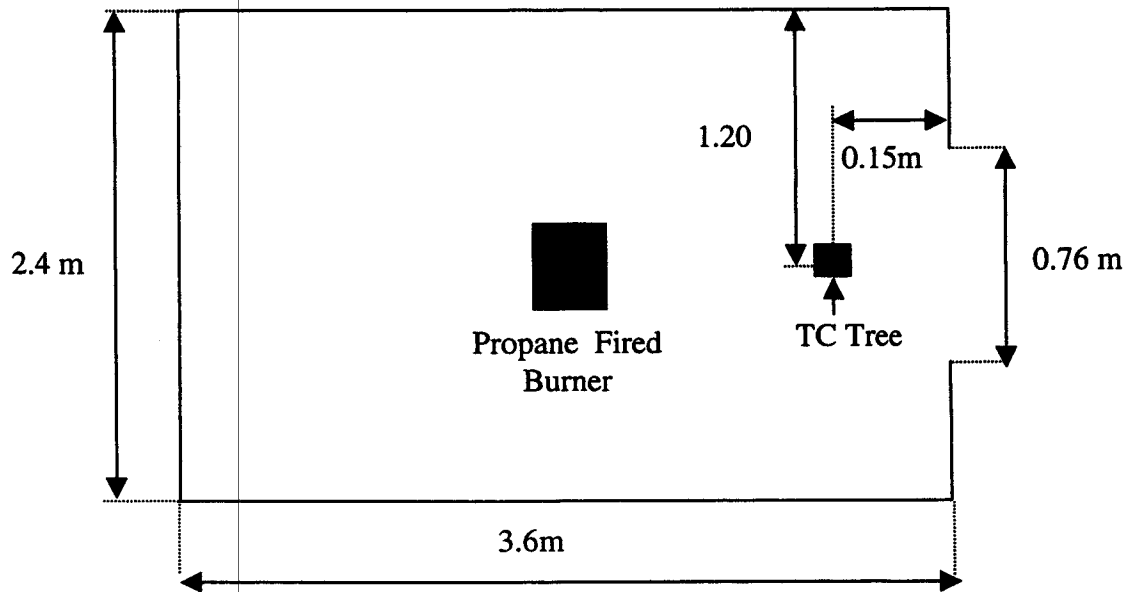


Figure 9: Plan view of compartment configuration #1, ceiling height 2.4m, and doorway height 2.0m, showing position of gas burner and thermocouple tree.

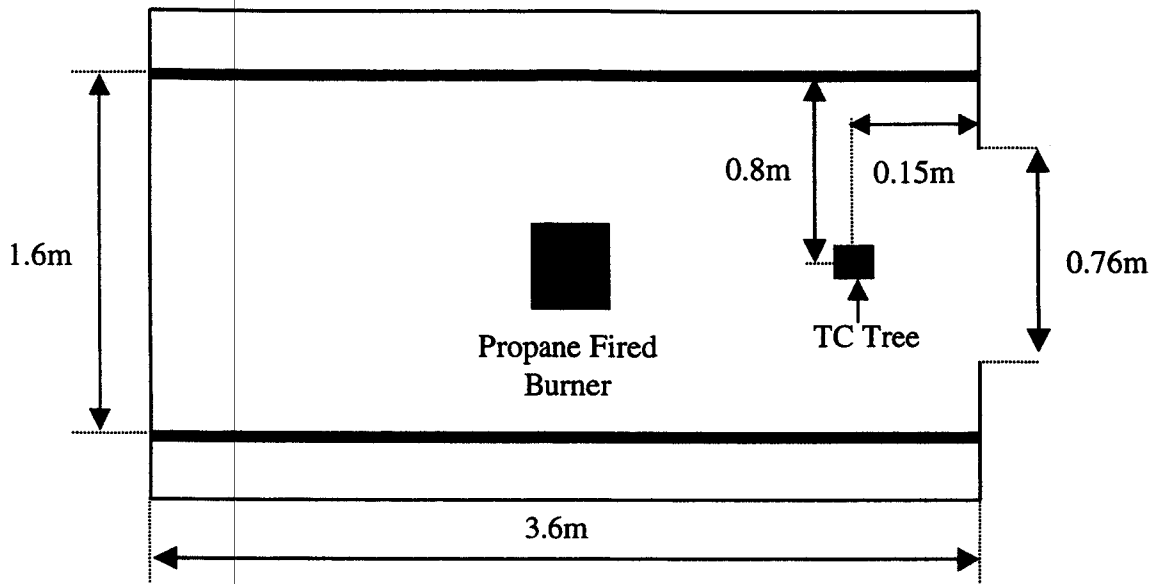


Figure 10: Plan view of compartment configuration #2, ceiling height 2.4m, and doorway height 2.0m, showing position of gas burner and thermocouple tree. Heavy lines indicate the new walls added to change the dimensions of the compartment.

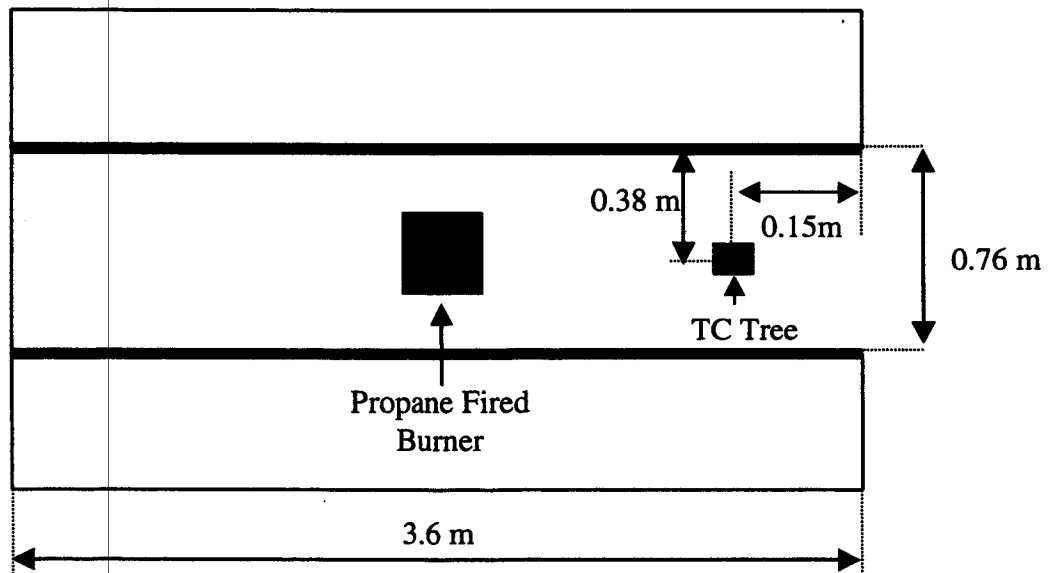


Figure 11: Plan view of compartment configuration #3, ceiling height 2.4m, and doorway height 2.0m, showing position of gas burner and thermocouple tree. Heavy lines indicate the new walls added to change the dimensions of the compartment.

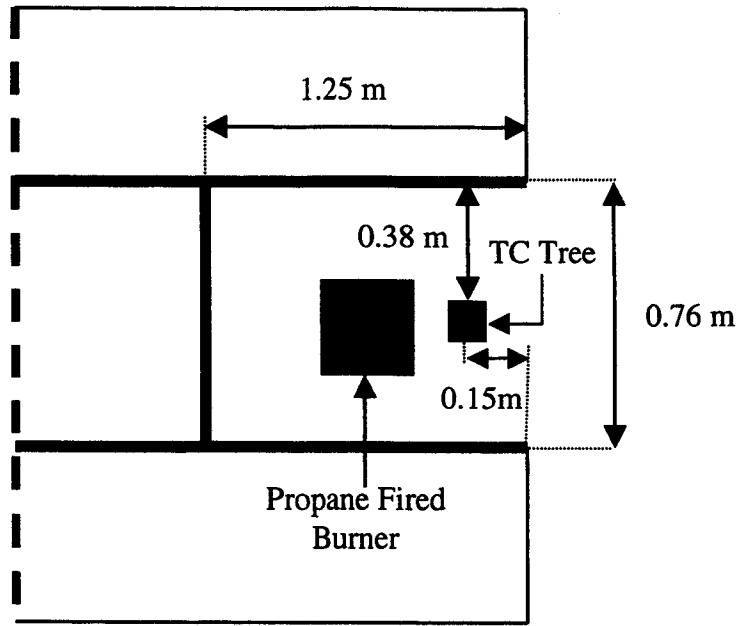


Figure 12: Plan view of compartment configuration #4, ceiling height 2.4m, and doorway height 2.0m, showing position of gas burner and thermocouple tree. Heavy lines indicate the new walls added to change the dimensions of the compartment. The dotted line indicates a cutoff of the rest of the compartment.

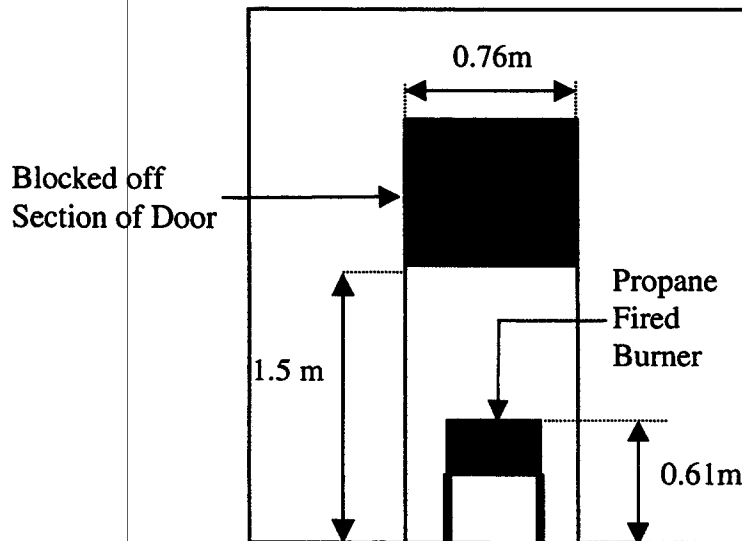


Figure 13: Front view of compartment configuration #5, plan is the same as compartment configuration #4 with the ceiling height lowered to 1.5m. There is no soffet on the door. The burner was still located in the center of the room with the thermocouple tree located between the burner and the door.

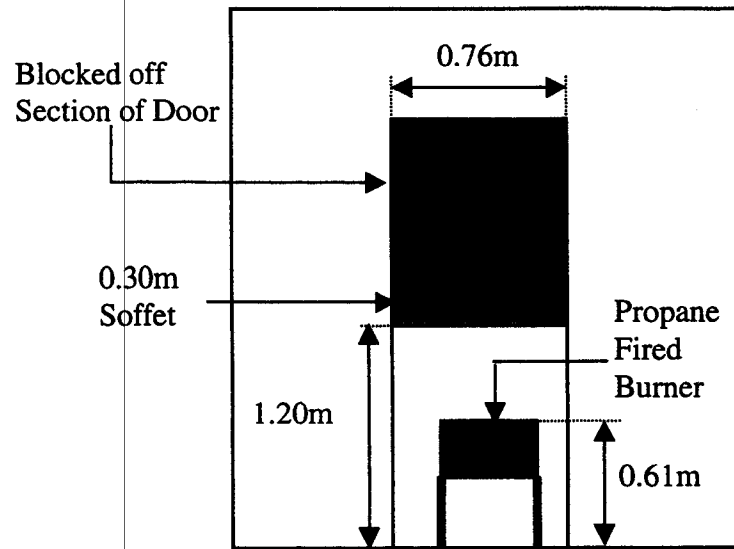


Figure 14: Front view of compartment configuration #6, plan is the same as compartment configuration #4, ceiling height 1.5m with a 0.3m soffet on the door. The burner was still located in the center of the room with the thermocouple tree located between the burner and the door.

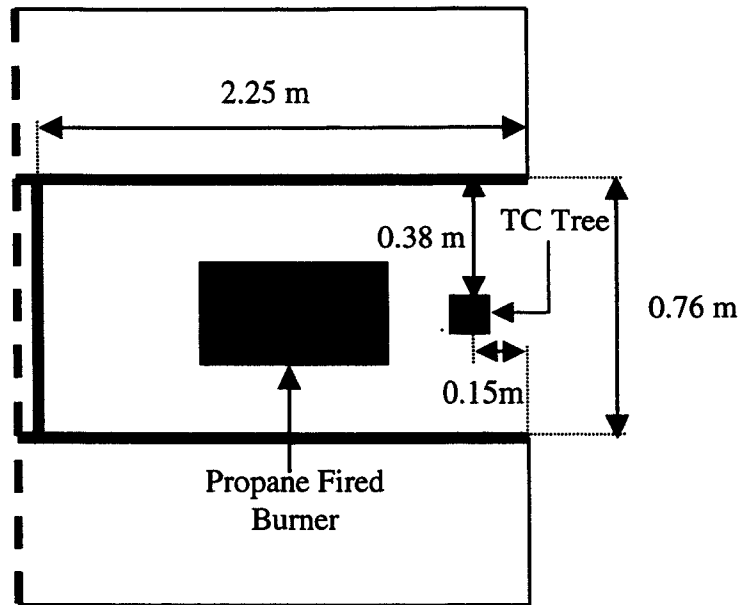


Figure 15: Plan view of compartment configuration #7, the front view was the same as compartment configuration #6 ceiling height 1.5m, and doorway height 1.2m, which was used for the experiments with the rectangular burner. Heavy lines indicate the new walls added to change the dimensions of the compartment. The dotted line indicates a cutoff of the rest of the compartment.

5.0 Experimental Data

A summary of the flame height data from all experiments can be found in Table 4. For each experiment conducted the table provides information including the hydraulic diameter of the burner, the HRR and the non-dimensional HRR of the fire, the 50% intermittency flame height, the 50% intermittency flame height normalized by the hydraulic diameter of the burner, the slope of the intermittency curve divided by the 50% intermittency flame height and Pagni's¹¹ flame puffing correlation.